ACS OMEGA

http://pubs.acs.org/journal/acsodf

Article

Exploration of ^{68}Ga-DOTA-MAL as a Versatile Vehicle for Facile Labeling of a Variety of Thiol-Containing Bioactive Molecules

Zhan Si,[‖] Yuan Cheng,[‖] Zhan Xu, Dai Shi, Hongcheng Shi,* and Dengfeng Cheng*

Cite This: *ACS Omega* 2023, 8, 4747−4755

Read Online

ACCESS | Metrics & More | Article Recommendations | Supporting Information

ABSTRACT: Efficient and site-specific radiolabeling reactions are essential in molecular probe synthesis. Thus, selecting an effective method for radiolabeling that does not affect bioactivity of the molecule is critical. Varieties of bifunctional chelating agents provide a solution in this matter. As a chemo-specific chelator, maleimido-mono-amide-DOTA (DOTA-Mal) holds significant potential for ^{68}Ga labeling of bioactive molecules; it can react specifically with free sulfhydryl groups under mild conditions. Compared with amino and carboxylic acid groups, free sulfhydryl groups are relatively less common in most biomolecules and can serve as site-specific radiolabeling targets. Labeling of ^{68}Ga usually employs a two-step labeling strategy; first, chelators are conjugated to the biomolecules, which is followed by radiolabeling. However, the bioactivity of biomolecules may be affected by harsh labeling conditions. In this study, three ^{68}Ga-labeled bioactive molecules, namely, ^{68}Ga-DOTA-RGD, ^{68}Ga-DOTA-FA, and ^{68}Ga-DOTA-BSA, were prepared using a novel strategy under mild conditions (pH of 8.0 at room temperature). Using this strategy, DOTA-Mal was labeled by ^{68}Ga before it reacted with the sulfhydryl group−containing biomolecules, which avoided damage to said biomolecules caused by the harsh reaction conditions required in ^{68}Ga-labeling procedures. The biological and chemical properties of these three radiotracers synthesized using this strategy are well manifested. Through a series of experiments, the effectiveness of this strategy is demonstrated, and we believe that this site-specific bioactivity-friendly reaction strategy will facilitate developments and translation applications of varieties of ^{68}Ga-labeled positron emission tomography probes.

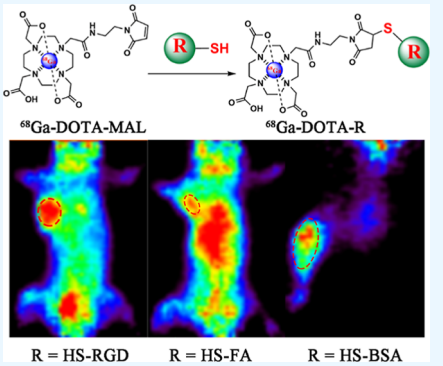

INTRODUCTION

Precision medicine is becoming a widely accepted guide to the action in the medical field, and its realization depends upon accuracy in the recognition of different targets.[1] As a non-invasive imaging modality, positron emission tomography (PET) plays an important role in precision medicine given its unparalleled advantages in the identification of molecular targets and the visualization of biological processes.[2,3] The value of PET is also embodied in the ability to assess the in vivo distribution and pharmacokinetics of medicine by labeling appropriate positron-emitting nuclides.[4]

^{18}F-fluorodeoxyglucose (^{18}F-FDG) is the most widely used radiotracer for PET imaging today; however, it has been hampered by well-described limitations (e.g., a lack of specificity) when applied to precision medicine.[5,6] In this context, a series of specific PET molecular probes labeled with different nuclides have been gradually developed for the assessment of specific biomarkers involved in different diseases and signaling pathways.[5,7,8]

During the development of radiopharmaceuticals, how to select an appropriate nuclide is the problem that must be considered. As the most commonly used positron-emitting nuclide, ^{18}F can be labeled to biomolecules using a direct labeling method; however, this process often requires rigorous conditions that may result in inactivation and degradation of the biomolecules.[9] Therefore, numerous ^{18}F-labeled prosthetic groups for peptide and protein conjugates have been developed. Unfortunately, this indirect labeling method is laborious to use.[10] Other positron nuclides already applied in clinical trials include ^{11}C, ^{89}Zr, and ^{124}I; however, each of these also has its own disadvantages that prevent further application, such as the short half-life of ^{11}C, the osteophilic property of ^{89}Zr, and instability of ^{124}I-labeled probes.[7,11−13] Moreover, the production of all the above nuclides requires an expensive on-site cyclotron, which undoubtedly further limits their applications. Recently, inspired by the successful clinical use of ^{68}Ga-labeled bioactive molecules such as ^{68}Ga-DOTA-TATE, ^{68}Ga-FAPI, and ^{68}Ga-PSMA, ^{68}Ga-labeled diagnostic tracers have become a hotspot in the design of biomedical imaging probes.[14−16] Compared to other clinically available short-lived positron emitters (^{11}C and ^{18}F), ^{68}Ga exhibits some unique characteristics that make it attractive, including suitable

Received: October 18, 2022
Accepted: January 19, 2023
Published: January 27, 2023

nuclear decay properties for PET imaging (β^+ 0.74 MeV, 89% abundance, $t_{1/2}$ = 67.7 min), generator production, commercially available chelators, and the potential to form a theranostic pair with ^{177}Lu/^{90}Y.[11,17]

The development of effective bifunctional chelators has broadened the application prospects of metal nuclides in nuclear medicine. Numerous literature studies have described the process of radiolabeling biomolecules using bifunctional chelators, which are first conjugated to biomolecules via primary amino groups and then followed by radiolabeling.[18,19] However, this approach cannot satisfy all situations effectively. (1) When the labeled substrates that are not commercialized or need to be extracted from patients, the conjugation of the active ester and primary amine is usually carried out under weak alkaline conditions, while the radiolabeling of ^{68}Ga often occurs in an acidic environment, the replacement of the buffer system is inevitable. This is a time-consuming and labor-intensive process, which may impair the biological activity and solubility of the prepared probes.[10,20] (2) Although we can radiolabel ^{68}Ga at room temperature using NOTA, DOTA is the "gold standard" for a series of therapeutic isotopes, and the high temperatures required for the labeling of radionuclides using DOTA as a chelating agent may damage the activities of biomolecules (especially for macromolecular proteins).[21] (3) Moreover, under normal conditions, the conjugation site of biomolecules to the chelating agents is random and may cause the active center to be modified, which will impair the affinity and specificity of prepared radiopharmaceuticals.[9,11] Compared to primary amine and other reactive functional groups, the sulfhydryl group particularly prone to reaction with sulfhydryl reagents (such as maleimide derivative, a bifunctional chelator for metal radionuclides) under physiological conditions are rare in biomolecules, and this property provides a highly chemo-selective labeling site when designing radiopharmaceuticals.[22,23]

Derivatives of maleimide have been used for the labeling of ^{68}Ga. When labeling ^{68}Ga using maleimido-mono-amide-DOTA (DOTA-Mal), a two-step process is followed; first, the chelators are conjugated to the biomolecules, and then ^{68}Ga labeling is performed, which also requires the biomolecules to be heated. In our proof-of-principle study, we improved this two-step labeling method, and three ^{68}Ga-labeled molecular probes were prepared using the new method. Afterward, a series of biological experiments were performed using these three molecular probes to judge the feasibility of this new method. The purpose of this article is to introduce a new candidate or complementary labeling strategy, which we hope can provide some assistance in the labeling of biomolecules that are inconvenient to be labeled using conventional methods.

EXPERIMENTAL SECTION

General. ^{68}Ga was eluted from a ^{68}Ge/^{68}Ga isotope generator (itG, Munich, Germany) with 0.05 M HCl. The sulfhydryl-modified RGD peptide and folate (HS-^{2K}PEG-FA) were obtained from Ruixi Biotechnology (Xi'an, China). Maleimide-mono-amide-DOTA (DOTA-Mal) was purchased from Macrocyclics (Richardson, TX, USA). All solvents used for radio-high-performance liquid chromatography (radio-HPLC) analysis in this study were of HPLC-grade. All other solvents and reagents were of analytical grade, while no further purification was performed. Water was distilled and deionized (918.2 MΩ/cm) using a Mili-Q water filtration system (Millipore, Burlington, MA, USA). All labeled biomolecules were purified using a pre-equilibrated PD-10 desalting column (GE Healthcare, Chicago, IL, USA), while phosphate-buffered saline (PBS) was used as the eluent. Radio-HPLC analyses were conducted using a size-exclusion column (Superose 12 10/300 GL; GE Healthcare) and performed on a 1260 Infinity HPLC system (Agilent Technologies, Santa Clara, CA, USA).

Radiochemistry. *Preparation of the ^{68}Ga-DOTA-Mal.* Briefly, 50 μg of DOTA-Mal was dissolved in 0.6 mL of NaOAc buffer (0.25 M, pH, 5.5) in an ampoule reactor with 2.4 mL of freshly eluted $^{68}GaCl_3$. After incubation for 10 min at 95 °C with continuous stirring, the mixture was passed through a 0.22 μm pore-size filter (Millipore, Burlington, MA, USA) and stored temporarily in the sterile vial for later use.

Preparation of the ^{68}Ga-DOTA-RGD. For the preparation of ^{68}Ga-DOTA-RGD, 0.825 μmol of TCEP [tris(2-carboxyethyl)phosphine] (1.5 equiv) was added to 0.1 mL of PBS (pH, 7.4) containing 400 μg of thiol RGD peptide and incubated for 5 min at room temperature (RT). Meanwhile, 75 μL of 20× PBS (0.2 M pH 7.4) was added to ^{68}Ga-DOTA-Mal solution, and the pH was adjusted to 7.4−8.3 using 0.5 M NaOH. Then, the TCEP-reduced sulfhydryl RGD peptide (HS-RGD) was directly added to the ^{68}Ga-DOTA-Mal solution and incubated for 20 min at 37 °C with continuous stirring. ^{68}Ga-DOTA-RGD was collected after purification using a pre-equilibrated PD-10 desalting column.

Preparation of the ^{68}Ga-DOTA-FA. Likewise, ^{68}Ga-DOTA-FA was prepared following a similar protocol. The HS-FA was reduced using 0.225 μmol of TCEP (1.5 equiv) and, after the pH value of ^{68}Ga-DOTA-Mal solution was adjusted to 7.4−8.3 by 20× PBS and 0.5 mol/L of NaOH, the TCEP-treated reduction products were added into the ^{68}Ga-DOTA-Mal solution. The resulting solution was stirred continuously for 20 min at 37 °C. After purification with a pre-equilibrated PD-10 desalting column, ^{68}Ga-DOTA-FA was collected.

Preparation of the ^{68}Ga-DOTA-BSA. For the preparation of ^{68}Ga-DOTA-BSA, 0.1 mM (6.7 g) of bovine serum albumin (BSA) in 0.1 M HEPES buffer (pH, 8.3) was incubated with 0.3 of mM dithiothreitol (DTT) for 90 min at RT. The reduction product was dialyzed thoroughly in the distilled and deionized water (DDW) to remove excess DTT at RT. After purification, the DTT-treated BSA (HS-BSA) 67 mg was added to the ^{68}Ga-DOTA-Mal solution and the mixture was incubated for 30 min at 37 °C under continuous magnetic stirring. After purification with a pre-equilibrated PD-10 desalting column, ^{68}Ga-DOTA-BSA was collected.

Cell Cultures and Model Constructions. Human gastric cancer (MGC-803) and ovarian carcinoma (SKOV-3) cell lines were purchased from Zhongqiaoxinzhou Biotech (Shanghai, China) and cultured with the recommended medium [DMEM cell culture medium supplemented with 10% fetal bovine serum (FBS)] at 37 °C in humidified air with 5% carbon dioxide and then kept in the logarithmic growth phase. Female ICR mice and BALB/c nude mice (4−5 weeks of age) were purchased from JieSiJie Laboratory Animal Co. (Shanghai, China) and raised under specific pathogen-free conditions. Inflammation models were constructed by the subcutaneous injection of turpentine oil (30 μL) in the right thigh, while xenograft models were constructed by subcutaneous injection of 100 μL of the cell suspension (with 5×10^6 of MGC-803 or SKOV-3 cells in PBS) on the right shoulder. All animal studies were performed following the guidelines

https://doi.org/10.1021/acsomega.2c06720
ACS Omega 2023, 8, 4747−4755

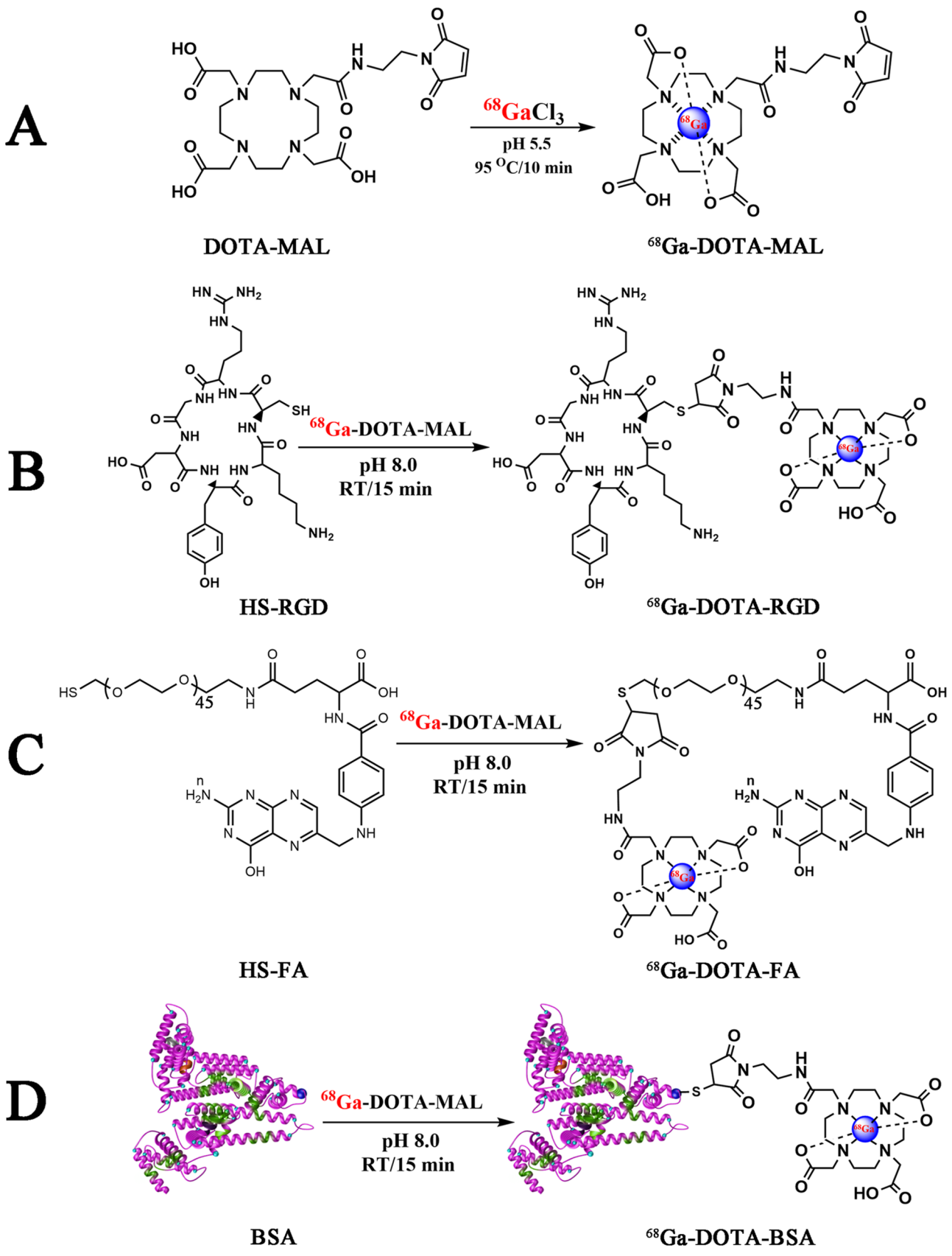

Figure 1. (A–D) Radiosynthesis of ^{68}Ga-DOTA-MAL, ^{68}Ga-DOTA-RGD, ^{68}Ga-DOTA-FA, and ^{68}Ga-DOTA-BSA.

approved by the Animal Care Committee of Fudan University (Shanghai, China).

Radiochemical Purity and Stability Testing. To analyze the radiochemical purity of the prepared radiotracers; after purification, 100 μL of each product solution was analyzed by

https://doi.org/10.1021/acsomega.2c06720
ACS Omega 2023, 8, 4747−4755

size-exclusion high performance liquid chromatography (SEC-HPLC). The in vitro stability of all three radiotracers was analyzed by instant thin-layer chromatography (iTLC) after incubation in 1× PBS or 10% FBS for 0, 30, 60, 120, and 180 min. The incubated radiotracers were then added to silica-gel chromatography paper (SGI0001; Agilent Technologies) strips, and we used 0.1 M sodium hydroxide as the mobile phase.

Biodistribution Studies. MGC-803 and SKOV-3 tumor-bearing mice were injected with 10 MBq of ^{68}Ga-DOTA-RGD (740 MBq/μmol) and ^{68}Ga-DOTA-FA (555 MBq/μmol), respectively; then were executed at 60 and 180 min after injection, and their pre-selected tissues and organs (including blood, liver, kidneys, spleen, heart, lungs, tumor, brain, muscle, and intestines) were collected. For blocking studies, the radiotracers were co-injected with the excess of unlabeled sulfhydryl RGD peptide (50 mg/kg of mouse body weight, i.e., 3 MBq/μmol) or unlabeled sulfhydryl folate (80 mg/kg of mouse body weight, i.e., 10 MBq/μmol), and the mice were executed at 180 min after injection. The collected tissues and organs were put into pre-weighed tubes. After being weighted, the radioactivity of all samples was measured using an automatic gamma counter (GC-1200, Zonkia Scientific Instruments Co., Ltd., Hefei, China).

The biodistribution assay of ^{68}Ga-DOTA-BSA was performed on the inflammation models following a similar protocol. Briefly, at 30 and 60 min after injection of 5−10 MBq of ^{68}Ga-DOTA-BSA (130 MBq/μmol), the mice were executed under anesthesia, and the blood, liver, kidneys, spleen, heart, lungs, inflamed tissue, brain, muscle, and intestines were collected. After being weighted and counted, the radioactivity uptake was calculated and presented as the percent injected dose per gram of tissue (% ID/g), and data were presented as histograms.

Pharmacokinetics. The pharmacokinetics experiences of the ^{68}Ga-labeled RGD (740 MBq/μmol), FA (555 MBq/μmol), and BSA (130 MBq/μmol) were assessed among female ICR mice (6−8 weeks of age, n = 4 for each group). The mice in each group were injected with 5 MBq of radiotracers via the tail vein. Blood samples (10−15 μL) were collected at 1, 3, 5, 10, 15, 30, 45, 60, 90, and 120 min after injection. After being counted and weighted, the sample's radioactivity was presented as % ID/g and analyzed using a two-compartment model.

Micro-PET Imaging. Micro-PET imaging was performed on a Focus Madiclab Metis 1800 micro-PET scanner (Madic Technology Co. Ltd., Linyi, China). To obtain the highest image resolution and sensitivity, the mice were placed in the center of the field of view (FOV). When the tumor reached 800−1000 mm^3 in size, MGC-803 and SKOV-3 tumor-bearing mice were injected with 10−15 MBq of ^{68}Ga-DOTA-RGD (740 MBq/μmol) or ^{68}Ga-DOTA-FA (555 MBq/μmol) via the tail vein, respectively. To prove that this labeling method does not affect the biological activity of the molecule, blocking experiments were performed using co-injected excess sulfhydryl RGD (1.3 mg, i.e., 3 MBq/μmol) or sulfhydryl FA (2.0 mg, i.e., 10 MBq/μmol) with labeled radiotracers. For the inflammation model, 10−15 MBq of ^{68}Ga-DOTA-BSA (130 MBq/μmol) was injected intravenously at 14 days after injection of turpentine oil. The mice were anesthetized and fixed in the prone position before PET scanning. For ^{68}Ga-DOTA-RGD and ^{68}Ga-DOTA-FA, the raw data were acquired at 1 and 3 h after injection, and the raw data for ^{68}Ga-DOTA-BSA were acquired at 0.5 and 1 h after injection. Static PET's data-collection process lasted 30 min for each scanning, and the images were reconstructed using the Research Workspace software (Mediclab, Houston, TX, USA).

Histological Examination. After imaging, all mice were sacrificed, and their tumors, inflamed tissues, and muscles were harvested immediately. All samples were fixed in formalin for 24 h; after dehydration and embedding, each paraffin-embedded tissue was sliced into 5 μm sections. The slices were dewaxed and rehydrated before hematoxylin and eosin (H&E) staining.

Statistical Analysis. All data are presented as mean or mean ± standard deviation values. All studies were repeated ≥3 independent times. The data analysis and statistical calculations were performed in the GraphPad Prism software (version 8.02; GraphPad Software, La Jolla, CA, USA). A difference was statistically significant when $P \leq 0.05$.

RESULTS

Radiochemistry. For ^{68}Ga-DOTA-Mal, the decay-corrected labeling yield ranged from 92 to 95% after passing through a 0.22 μm Millipore filter, while the radiochemical purity was >98% despite being unpurified. After purification using pre-equilibrated PD-10 desalting columns, ^{68}Ga-DOTA-RGD, ^{68}Ga-DOTA-FA (folic acid), and ^{68}Ga-DOTA-BSA (albumin) were obtained with yields of 90%, 85%, and 20%, respectively (Figure 1A−D). Radio-HPLC analysis showed that the radiochemical purities for these radiotracers were all close to 100% (Figure 2). The mean specific activities of ^{68}Ga-DOTA-RGD, ^{68}Ga-DOTA-FA, and ^{68}Ga-DOTA-BSA were 740, 555, and 130 MBq/μmol, respectively. The in vitro stabilities of these three radiotracers were analyzed using iTLC. As shown in Figures 3 and S1, after being incubated in PBS or FBS, all these radiotracers exhibited excellent stabilities.

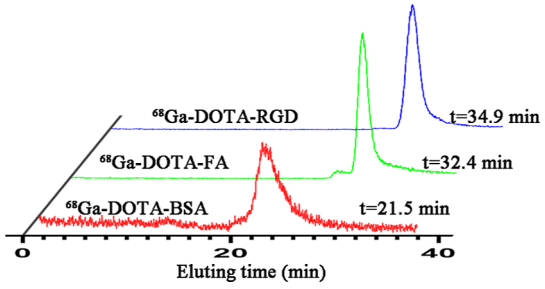

Figure 2. Radio-HPLC analysis of ^{68}Ga-DOTA-RGD, ^{68}Ga-DOTA-FA, and ^{68}Ga-DOTA-BSA.

Biodistribution and Pharmacokinetics. The biodistribution experiences of ^{68}Ga-DOTA-RGD and ^{68}Ga-DOTA-FA were performed on the MGC-803 ($\alpha_v\beta_3$-positive Human gastric cancer MGC-803 cell lines) or SKOV-3 (FA-positive ovarian cancer SKOV-3 cell lines) tumor-bearing BALB/c nude mice, while the biodistribution experience of ^{68}Ga-DOTA-BSA was performed on inflammation models.

As shown in Figure 4A, for ^{68}Ga-DOTA-RGD, the radioactivity of MGC-803 tumors at 1 and 3 h after injection were 4.31 ± 0.93% and 8.30 ± 0.92% ID/g, respectively. When blocked by co-injected HS-RGD, the uptake of ^{68}Ga-DOTA-RGD in MGC-803 tumors was reduced significantly from 8.30 ± 0.92% ID/g to 1.53 ± 0.40% ID/g at 3 h after injection (P < 0.05). ^{68}Ga-DOTA-RGD is mainly metabolized through the

https://doi.org/10.1021/acsomega.2c06720
ACS Omega 2023, 8, 4747−4755

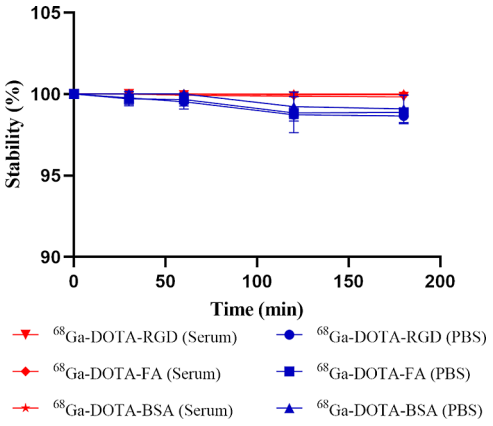

Figure 3. In vitro stability of ^{68}Ga-DOTA-RGD, ^{68}Ga-DOTA-FA, and ^{68}Ga-DOTA-BSA in 1× PBS or 10% FBS.

liver and kidneys. Compared to biodistribution at 1 h after injection, the accumulation of ^{68}Ga-DOTA-RGD was significantly decreased at 3 h in most tissues and organs (all $P < 0.05$). Furthermore, at 3 h after injection, the uptake of ^{68}Ga-DOTA-RGD in tumors exceeded that in the intestines, with the highest radioactive uptake occurring at 1 h after injection.

For ^{68}Ga-DOTA-FA, the radioactivities of SKOV-3 at 1 and 3 h after injection were 5.62 ± 1.58% and 13.36 ± 2.86% ID/g, respectively (Figure 4B). In the blocking group, the uptake of ^{68}Ga-DOTA-FA in SKOV-3 tumors was reduced significantly from 13.36 ± 2.86% ID/g to 1.89 ± 0.11% ID/g ($P < 0.05$). In folate receptor (FR)-positive organs, such as the kidneys, the uptake of ^{68}Ga-DOTA-FA gradually increased from 4.38 ± 1.27% ID/g to 5.56 ± 1.40% ID/g at 3 h after injection. However, 3 h post-injection, the radioactivity of ^{68}Ga-DOTA-FA in SKOV-3 tumors was 13.36 ± 2.86% ID/g, which was much higher than those in the kidneys and blood (5.56 ± 1.40% ID/g and 7.20 ± 1.29% ID/g). Figure 4C shows that the uptakes of ^{68}Ga-DOTA-BSA in inflammatory tissues at 0.5 and 1 h after injection were 4.32 ± 1.10% and 6.50 ± 0.40% ID/g, respectively.

All three radiotracers in ICR mouse blood showed a fast clearance curve, with a short half-life, as presented in Figure 5. The goodness-of-fit (r^2) values, rate constants for distribution and elimination (k_α, k_β), and distribution and elimination half-lives for each radiopharmaceutical are presented in Table 1.

Micro-PET Imaging and HE Staining. For micro-PET imaging, a 30 min static scanning was performed on the MGC-803 and SKOV-3 tumor-bearing mice following the injection of ^{68}Ga-DOTA-RGD or ^{68}Ga-DOTA-FA. PET imaging data were acquired at 1 and 3 h after the injection of each radiotracer (Figure 6A). For ^{68}Ga-DOTA-RGD, MGC-803 tumors showed an obvious tracer uptake at 1 h after injection, which changed insignificantly even at 180 min. In contrast to tumor cells, most of the radioactivity in normal tissues and organs was cleared within 180 min after injection, which resulted in a much higher tumor-to-background contrast (the tumor-to-muscle ratios were 3.13 ± 0.15 and 4.46 ± 0.40 at 1 and 3 h after injection). For ^{68}Ga-DOTA-FA, the FR expression level of SKOV-3 tumors was visualized using PET scanning at 1 and 3 h after injection (Figure 6B). In most normal tissues and organs, the accumulation of tracers decreased rapidly with time, but the radioactivity in the intestines and kidneys was significantly higher at 3 h after injection than at 1 h. The uptake of both radiotracers in tumor-

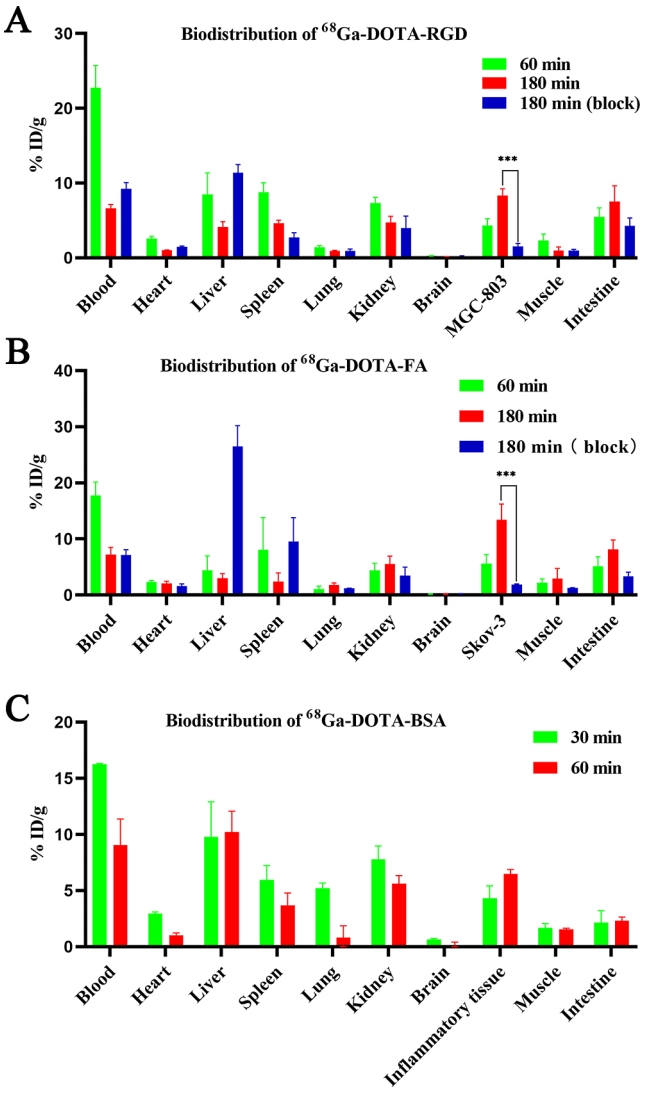

Figure 4. (A) Biodistribution of ^{68}Ga-DOTA-RGD in the MGC-803 tumor bearing mice at 60 and 180 min after injection with or without excess unlabeled precursor (n = 3); (B) biodistribution of ^{68}Ga-DOTA-FA in the SKOV-3 tumor bearing mice at 60 and 180 min after injection with or without excess unlabeled precursor (n = 3); and (C) biodistribution of ^{68}Ga-DOTA-BSA in the inflammation model at 30 and 60 min after injection (n = 3). Data are shown as mean ± SD, ***$P < 0.001$.

bearing mice could be blocked by co-injecting with excess unlabeled precursors. The feasibility of specific imaging for inflamed tissues using ^{68}Ga-DOTA-BSA was also evaluated using micro-PET, and the results showed that the inflamed tissue was recognized easily by distinct accumulation of radiotracers at 0.5 and 1 h after injection (Figure 7). All three radiotracer imaging results were consistent with biodistribution studies. H&E staining showed different histological features between tumors and muscles (Figure 8).

DISCUSSION

At present, in addition to the conventional random conjugation based on lysine and activated esters, several novel conjugation strategies have shed light on the construction of imaging probes.[11] Since the concept of click chemistry was proposed, it has put a profound impact on radiochemistry, especially on the preparing of radiopharma-

https://doi.org/10.1021/acsomega.2c06720
ACS Omega 2023, 8, 4747−4755

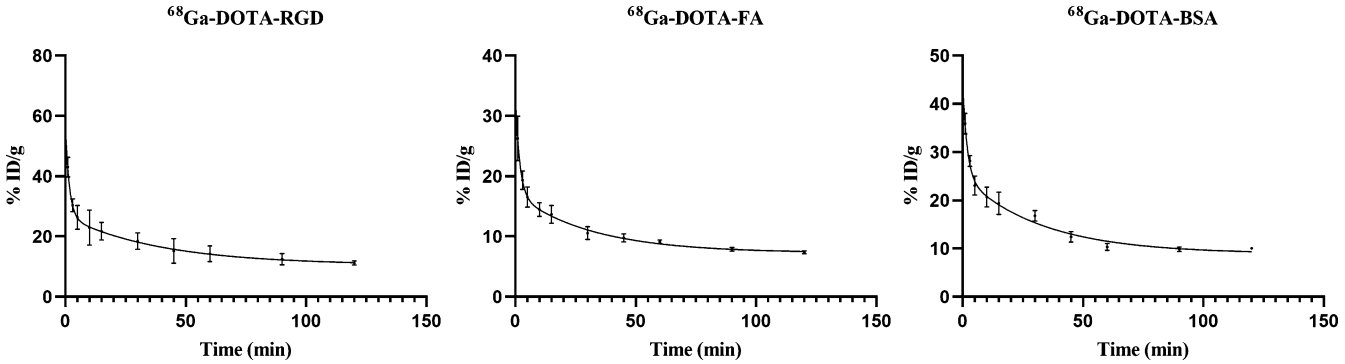

Figure 5. Pharmacokinetic results of different radiotracers.

Table 1. Pharmacokinetic Results of Different Radiotracers (n = 4)

parameter	Ga-68 folate	Ga-68 albumin	Ga-68 RGD	Ga-68 DOTA-MAL
r^2	0.9450	0.9673	0.9123	0.9592
k_α (min^{-1})	0.56 ± 0.15	0.77 ± 0.43	0.65 ± 0.11	0.93 ± 0.27
k_β (min^{-1})	0.03 ± 0.01	0.03 ± 0.01	0.02 ± 0.01	0.1 ± 0.04
$t_{1/2\alpha}$ (min)	1.33 ± 0.32	1.22 ± 0.65	1.11 ± 0.22	0.82 ± 0.26
$t_{1/2\beta}$ (min)	23.7 ± 5.71	25.09 ± 5.06	30.82 ± 8.59	8.08 ± 2.76

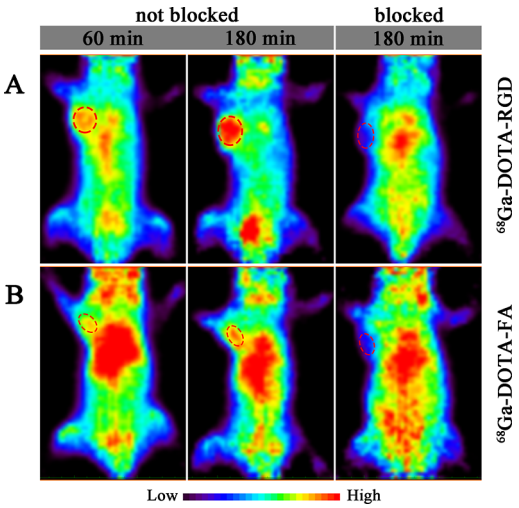

Figure 6. (A) Coronal micro-PET images of MGC-803 tumor bearing mice acquired at 60 and 180 min after injection of ^{68}Ga-DOTA-RGD with or without unlabeled RGD and (B) coronal micro-PET images of SKOV-3 tumor bearing mice acquired at 60 and 180 min after injection ^{68}Ga-DOTA-FA with or without unlabeled FA.

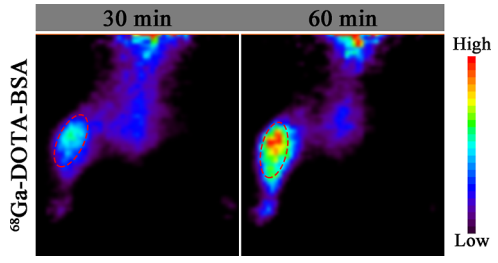

Figure 7. Coronal micro-PET images of inflammation model at 30 and 60 min after injection of ^{68}Ga-DOTA-BSA.

ceuticals. It is worth mentioning that as a bio-orthogonal click chemistry reaction, IEDDA has been widely used in pretargeted tumor imaging and radiotherapy due to its low immunogenicity, improved T/B ratios, and without blocking effects.[24,25] Apart from that, the photochemical and enzymatic methods have also come into light.[26,27] Nonetheless, site-selective bioconjugation via cysteine to maleimide remains one of the most popular options. Two FDA-approved drugs, Brentuximab vedotin and trastuzumab emtansine, have prepared successfully using this approach to target CD30 and HER2, respectively.[28] As a bifunctional chelator, DOTA-Mal, a member of the maleimide-based prosthetic group, is commonly used for radionuclide labeling. When using DOTA-Mal for ^{68}Ga labeling, the most common practice is to first conjugate the DOTA-Mal to the desired labeled biomolecules and then perform the labeling of ^{68}Ga. However, the heating conditions required may destroy the bioactivities of precursors. In this study, we successfully synthesized multiple ^{68}Ga-labeled radiotracers (including ^{68}Ga-DOTA-RGD, ^{68}Ga-DOTA-FA, and ^{68}Ga-DOTA-BSA) using DOTA-Mal by an improved labeling strategy, and the feasibility of this novel labeling method was proven through a series of biological experiments. The pharmacokinetic characteristics of prepared radiotracers are shown in Figure 5 and Table 1.

Integrin $\alpha_v\beta_3$ plays an important role in the promotion of angiogenesis, tumor growth, and metastasis. The high expression of $\alpha_v\beta_3$ in tumor cells makes it a suitable target for therapy, and $\alpha_v\beta_3$-based PET imaging is currently used in clinical tumor evaluation.[29] To demonstrate the bioactivities of ^{68}Ga-DOTA-RGD prepared by the new strategy, an MGC-803 subcutaneous tumor model, which has been well documented to have high $\alpha_v\beta_3$ expression, was used.[30] The biodistribution assay and PET imaging revealed a high uptake of ^{68}Ga-DOTA-RGD in tumors, and this uptake increased gradually over time, with the tumor-to-organ ratio peaking at 180 min after injection. The specificity of ^{68}Ga-DOTA-RGD was well demonstrated by a blocking experiment, and the tumor uptake of ^{68}Ga-DOTA-RGD was blocked by the co-injected HS-RGD significantly.

Similar to $\alpha_v\beta_3$, FR, which is a glycosylphosphatidylinositol-linked glycoprotein that mediates the endocytosis of folate and its derivatives, is also an important target for cancer diagnosis and treatment.[30] The prognosis of patients who are ready to

https://doi.org/10.1021/acsomega.2c06720
ACS Omega 2023, 8, 4747−4755

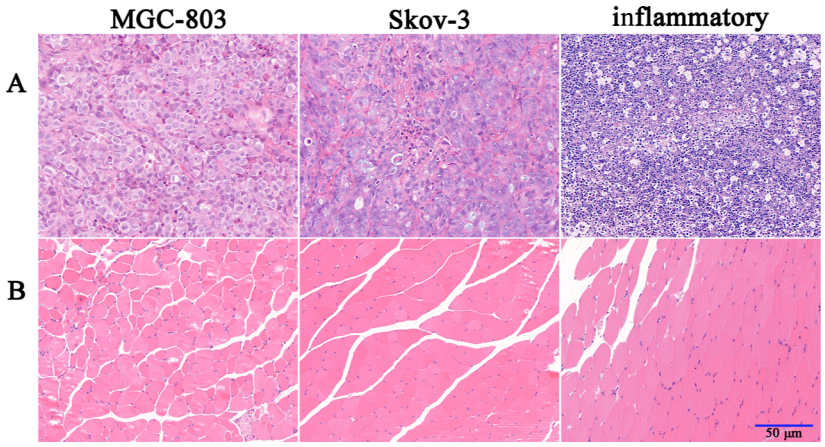

Figure 8. (A) H&E staining of MGC-803 tumor, SKOV-3 tumor, and inflamed tissue and (B) H&E staining of the normal muscle tissues in different models.

receive the related therapy will derive a benefit from the accurate quantification of FR expression levels. With this in mind, we constructed ^{68}Ga-DOTA-FA using the improved strategy for non-invasive monitoring of FR expression by PET imaging. Due to the high hydrophilicity of the polyethylene glycol (PEG)[31] chains, which minimized the non-specific binding of the radiotracer in vivo, PEGylation modification was carried out at the same time as thiol modification.[32] It was noted that, as shown in Figure 6B, the nuclide-labeled PEGylated FA could still bind to the receptor with high affinity. The results of the ex vivo biodistribution assay indicated that the ^{68}Ga-DOTA-FA mainly accumulated in the tumor, blood, kidneys, and intestines and was excreted through the hepatobiliary and urinary routes. Compared to other radiolabeled FA derivatives reported previously, the uptake of ^{68}Ga labeled PEGylated FA was significantly reduced in the kidneys, which can spare patients from the risk of renal radiation damage, especially those who are undergoing abdominal radiation therapy.[33]

Albumin (Alb) is the main component of plasm protein, accounting for 50−60% of the total plasm proteins in healthy adults. From the perspective of labeling, Alb represents a desirable system for several attributes, including stable and flexible molecular features, a series of hydrophobic cavities, and a free thiol group in the cysteine-34 residue.[34] Albumin exhibits passive accumulation properties in inflammatory diseases due to the enhanced permeability and retention effect of neovascularization, but this property has received little attention.[35] ^{68}Ga-DOTA-BSA was prepared using this highly chemo-selective and regio-selective approach, and the feasibility of this method when labeling macromolecules was proven by a series of in vivo studies performed on inflammation models. As shown in Figure 7, high accumulation of ^{68}Ga-DOTA-BSA in the inflamed tissue was observed on PET images at both time points, and uptake in inflammation lesions displayed an increasing trend over time. The radioactivity ratio between inflammatory lesions and muscles on PET images was consistent with biodistribution data.

As another commonly used positron nuclide, ^{18}F is also often labeled using prosthetic synthons, and maleimide derivatives have also been used. However, there are still some limitations to consider as follows: (1) such unlabeled prosthetic synthons are not directly available, and the preparation processes are confined to the chemists due to their complexity; (2) due to the short half-life of ^{18}F, the synthesis and labeling of such radiotracers are unfeasible at institutions without on-site cyclotrons; and (3) given the lability of some prosthetic synthons, when labeling them with ^{18}F, a three-step labeling method is usually required, which is a time-consuming process.[9,10] In contrast, pursuing the labeling of ^{68}Ga by DOTA-mal may be a better option for the following reasons: (1) DOTA-Mal chelator is a common reagent, making it relatively easy to obtain; (2) with the popularity of ^{68}Ge/^{68}Ga isotope generators, ^{68}Ga can be obtained more easily; and (3) by using the bifunctional chelator DOTA-Mal, ^{68}Ga can be labeled under mild conditions without compromising its thiol selectivity and allowing for direct radiolabeling.[17] Therefore, ^{68}Ga-DOTA-Mal would be a valuable alternative to ^{18}F-labeled prosthetic synthons for applications; particularly, as a hydrophilic bifunctional chelator, DOTA-Mal exhibits better water stability and nearly equal quantitative conjugation yields, and all of these desirable characteristics make it an appealing method.[36,37]

In addition to the regio-selectivity and chemo-selectivity mentioned previously, the improved labeling strategy also shows some other advantages. First, our labeling method carried out the chelation of radionuclides before linking chelator molecules containing nuclides to sulfhydryl-containing biomolecules that were intended to be labeled. This convenient reaction to label the bioactive molecules was performed in a neutral solution at RT, and when compared to the previous method that first conjugated the chelator to the biomolecule, the improved method significantly maintained the activity of biomolecules, especially for molecules which with high pH values and temperature sensitivity. Moreover, the conjugation reaction between the active ester and the bioactive molecule takes a longer time, which not only weakens the activity of the bioactive molecules but also complicates the purification process, and the introduction of DOTA-Mal can significantly speed up the process.

CONCLUSIONS

In this study, we synthesized multiple ^{68}Ga-labeled radiotracers using the bifunctional chelator DOTA-Mal, and the feasibility of using ^{68}Ga-DOTA-Mal to construct PET tracers with thiol-containing biomolecules was well proven via a series of biological experiments. Three PET probes, ^{68}Ga-DOTA-RGD, ^{68}Ga-DOTA-FA, and ^{68}Ga-DOTA-Mal-BSA, which were

https://doi.org/10.1021/acsomega.2c06720
ACS Omega 2023, 8, 4747−4755

labeled using this improved strategy, showed excellent stabilities and affinities, and their biological activities did not change significantly during these labeling processes. The entire radiolabeling process, including chelation, conjugation, and purification, took ≤40 min, and more importantly, using this strategy discards any possible unfriendly reaction conditions in the labeling process and helps to maintain the bioactivities of labeled molecules. In summary, we have reason to believe that ^{68}Ga-DOTA-MAL can be widely used to construct novel PET probes, and, to a certain extent, this strategy will promote the development of novel PET tracers.

■ ASSOCIATED CONTENT

Supporting Information

The Supporting Information is available free of charge at https://pubs.acs.org/doi/10.1021/acsomega.2c06720.

Radio-iTLC results of ^{68}Ga-DOTA-RGD, ^{68}Ga-DOTA-FA, and ^{68}Ga-DOTA-BSA (PDF)

■ AUTHOR INFORMATION

Corresponding Authors

Hongcheng Shi − *Department of Nuclear Medicine, Zhongshan Hospital and Institute of Nuclear Medicine, Fudan University, Shanghai 200032, China; Shanghai Institute of Medical Imaging, Shanghai 200032, China;* Email: shi.hongcheng@zs-hospital.sh.cn

Dengfeng Cheng − *Department of Nuclear Medicine, Zhongshan Hospital and Institute of Nuclear Medicine, Fudan University, Shanghai 200032, China; Shanghai Institute of Medical Imaging, Shanghai 200032, China;* orcid.org/0000-0003-2886-3273; Email: cheng.dengfeng@zs-hospital.sh.cn

Authors

Zhan Si − *Department of Nuclear Medicine, Zhongshan Hospital and Institute of Nuclear Medicine, Fudan University, Shanghai 200032, China; Shanghai Institute of Medical Imaging, Shanghai 200032, China;* orcid.org/0000-0001-8549-6604

Yuan Cheng − *Department of Nuclear Medicine, Zhongshan Hospital and Institute of Nuclear Medicine, Fudan University, Shanghai 200032, China; Shanghai Institute of Medical Imaging, Shanghai 200032, China*

Zhan Xu − *Department of Nuclear Medicine, Zhongshan Hospital and Institute of Nuclear Medicine, Fudan University, Shanghai 200032, China; Shanghai Institute of Medical Imaging, Shanghai 200032, China*

Dai Shi − *Department of Nuclear Medicine, Zhongshan Hospital and Institute of Nuclear Medicine, Fudan University, Shanghai 200032, China; Shanghai Institute of Medical Imaging, Shanghai 200032, China;* orcid.org/0000-0003-3903-5713

Complete contact information is available at: https://pubs.acs.org/10.1021/acsomega.2c06720

Author Contributions

‖Z.S. and Y.C. contributed equally to this paper.

Notes

The authors declare no competing financial interest.

■ ACKNOWLEDGMENTS

This study was funded by the National Nature Science Foundation of China (11875114, 82172002, 82171979, and 81871407), Shanghai Municipal Science and Technology Committee of Shanghai outstanding academic leaders plan (21XD1423500), the Training Program of Zhongshan Hospital of Fudan University (2020ZSLC20), and the Shanghai Municipal Key Clinical Specialty Project (SHSLCZDZK03401).

■ REFERENCES

(1) Pinker, K.; Chin, J.; Melsaether, A. N.; Morris, E. A.; Moy, L. Precision Medicine and Radiogenomics in Breast Cancer: New Approaches toward Diagnosis and Treatment. *Radiology* **2018**, *287*, 732−747.

(2) Wilson, H.; Politis, M.; Rabiner, E. A.; Middleton, L. T. Novel PET Biomarkers to Disentangle Molecular Pathways across Age-Related Neurodegenerative Diseases. *Cells* **2020**, *9*, 2581.

(3) Stendahl, J. C.; Kwan, J. M.; Pucar, D.; Sadeghi, M. M. Radiotracers to Address Unmet Clinical Needs in Cardiovascular Imaging, Part 2: Inflammation, Fibrosis, Thrombosis, Calcification, and Amyloidosis Imaging. *J. Nucl. Med.* **2022**, *63*, 986−994.

(4) Woo, S. K.; Jang, S. J.; Seo, M. J.; Park, J. H.; Kim, B. S.; Kim, E. J.; Lee, Y. J.; Lee, T. S.; An, G. I.; Song, I. H.; Seo, Y.; Kim, K. I.; Kang, J. H. Development of ^{64}Cu-NOTA-Trastuzumab for HER2 Targeting: A Radiopharmaceutical with Improved Pharmacokinetics for Human Studies. *J. Nucl. Med.* **2019**, *60*, 26−33.

(5) Sun, X.; Xiao, Z.; Chen, G.; Han, Z.; Liu, Y.; Zhang, C.; Sun, Y.; Song, Y.; Wang, K.; Fang, F.; Wang, X.; Lin, Y.; Xu, L.; Shao, L.; Li, J.; Cheng, Z.; Gambhir, S. S.; Shen, B. A PET imaging approach for determining EGFR mutation status for improved lung cancer patient management. *Sci. Transl. Med.* **2018**, *10*, No. eaan8840.

(6) Hao, L.; Rohani, N.; Zhao, R. T.; Pulver, E. M.; Mak, H.; Kelada, O. J.; Ko, H.; Fleming, H. E.; Gertler, F. B.; Bhatia, S. N. Microenvironment-triggered multimodal precision diagnostics. *Nat. Mater.* **2021**, *20*, 1440−1448.

(7) Zanotti-Fregonara, P.; Pascual, B.; Veronese, M.; Yu, M.; Beers, D.; Appel, S. H.; Masdeu, J. C. Head-to-head comparison of ^{11}C-PBR28 and ^{11}C-ER176 for quantification of the translocator protein in the human brain. *Eur. J. Nucl. Med. Mol. Imaging* **2019**, *46*, 1822−1829.

(8) Kwee, S. A.; Wong, L.; Chan, O. T. M.; Kalathil, S.; Tsai, N. PET/CT with ^{18}F Fluorocholine as an Imaging Biomarker for Chronic Liver Disease: A Preliminary Radiopathologic Correspondence Study in Patients with Liver Cancer. *Radiology* **2018**, *287*, 294−302.

(9) Wu, Z.; Li, L.; Liu, S.; Yakushijin, F.; Yakushijin, K.; Horne, D.; Conti, P. S.; Li, Z.; Kandeel, F.; Shively, J. E. Facile Preparation of a Thiol-Reactive ^{18}F-Labeling Agent and Synthesis of ^{18}F-DEG-VS-NT for PET Imaging of a Neurotensin Receptor-Positive Tumor. *J. Nucl. Med.* **2014**, *55*, 1178−1184.

(10) Ma, G.; McDaniel, J. W.; Murphy, J. M. One-Step Synthesis of ^{18}F-Fluoro-4-(vinylsulfonyl) benzene: A Thiol Reactive Synthon for Selective Radiofluorination of Peptides. *Org. Lett.* **2021**, *23*, 530−534.

(11) Wei, W.; Rosenkrans, Z. T.; Liu, J.; Huang, G.; Luo, Q. Y.; Cai, W. ImmunoPET: Concept, Design, and Applications. *Chem. Rev.* **2020**, *120*, 3787−3851.

(12) Mendler, C. T.; Friedrich, L.; Laitinen, I.; Schlapschy, M.; Schwaiger, M.; Wester, H. J.; Skerra, A. High contrast tumor imaging with radio-labeled antibody Fab fragments tailored for optimized pharmacokinetics via PASylation. *mAbs* **2015**, *7*, 96−109.

(13) Deri, M. A.; Zeglis, B. M.; Francesconi, L. C.; Lewis, J. S. PET imaging with ^{89}Zr: from radiochemistry to the clinic. *Nucl. Med. Biol.* **2013**, *40*, 3−14.

(14) Bodei, L.; Ambrosini, V.; Herrmann, K.; Modlin, I. Current Concepts in ^{68}Ga-DOTATATE Imaging of Neuroendocrine Neo-

https://doi.org/10.1021/acsomega.2c06720
ACS Omega 2023, 8, 4747−4755

plasms: Interpretation, Biodistribution, Dosimetry, and Molecular Strategies. *J. Nucl. Med.* **2017**, *58*, 1718−1726.
(15) Giesel, F. L.; Kratochwil, C.; Lindner, T.; Marschalek, M. M.; Loktev, A.; Lehnert, W.; Debus, J.; Jäger, D.; Flechsig, P.; Altmann, A.; Mier, W.; Haberkorn, U. ^{68}Ga-FAPI PET/CT: Biodistribution and Preliminary Dosimetry Estimate of 2 DOTA-Containing FAP-Targeting Agents in Patients with Various Cancers. *J. Nucl. Med.* **2019**, *60*, 386−392.
(16) Chavoshi, M.; Mirshahvalad, S. A.; Metser, U.; Veit-Haibach, P. ^{68}Ga-PSMA PET in prostate cancer: a systematic review and meta-analysis of the observer agreement. *Eur. J. Nucl. Med. Mol. Imaging* **2022**, *49*, 1021−1029.
(17) Satpati, D. Recent Breakthrough in ^{68}Ga-Radiopharmaceuticals Cold Kits for Convenient PET Radiopharmacy. *Bioconjugate Chem.* **2021**, *32*, 430−447.
(18) Shi, D.; Si, Z.; Xu, Z.; Cheng, Y.; Lin, Q.; Fu, Z.; Fu, W.; Yang, T.; Shi, H.; Cheng, D. Synthesis and Evaluation of ^{68}Ga-NOTA-COG1410 Targeting to TREM2 of TAMs as a Specific PET Probe for Digestive Tumor Diagnosis. *Anal. Chem.* **2022**, *94*, 3819−3830.
(19) Yang, J.; Xu, J.; Gonzalez, R.; Lindner, T.; Kratochwil, C.; Miao, Y. ^{68}Ga-DOTA-GGNle-CycMSH(hex) targets the melanocortin-1 receptor for melanoma imaging. *Sci. Transl. Med.* **2018**, *10*, No. eaau4445.
(20) Zhang, T.; Cai, J.; Wang, H.; Wang, M.; Yuan, H.; Wu, Z.; Ma, X.; Li, Z. RXH-Reactive ^{18}F-Vinyl Sulfones as Versatile Agents for PET Probe Construction. *Bioconjugate Chem.* **2020**, *31*, 2482−2487.
(21) Price, E. W.; Orvig, C. Matching chelators to radiometals for radiopharmaceuticals. *Chem. Soc. Rev.* **2014**, *43*, 260−290.
(22) Fay, R.; Holland, J. P. The Impact of Emerging Bioconjugation Chemistries on Radiopharmaceuticals. *J. Nucl. Med.* **2019**, *60*, 587−591.
(23) Ravasco, J.; Faustino, H.; Trindade, A.; Gois, P. M. P. Bioconjugation with Maleimides: A Useful Tool for Chemical Biology. *Chemistry* **2019**, *25*, 43−59.
(24) Zhang, Y.; Lin, Q.; Wang, T.; Shi, D.; Fu, Z.; Si, Z.; Xu, Z.; Cheng, Y.; Shi, H.; Cheng, D. Targeting Infiltrating Myeloid Cells in Gastric Cancer Using a Pretargeted Imaging Strategy Based on Bio-Orthogonal Diels-Alder Click Chemistry and Comparison with ^{89}Zr-Labeled Anti-CD11b Positron Emission Tomography Imaging. *Mol. Pharm.* **2022**, *19*, 246−257.
(25) Paganelli, G.; Chinol, M. Radioimmunotherapy: is avidin-biotin pretargeting the preferred choice among pretargeting methods? *Eur. J. Nucl. Med. Mol. Imaging* **2003**, *30*, 773−776.
(26) Patra, M.; Eichenberger, L. S.; Fischer, G.; Holland, J. P. Photochemical Conjugation and One-Pot Radiolabelling of Antibodies for Immuno-PET. *Angew. Chem., Int. Ed. Engl.* **2019**, *58*, 1928−1933.
(27) Alt, K.; Paterson, B. M.; Westein, E.; Rudd, S. E.; Poniger, S. S.; Jagdale, S.; Ardipradja, K.; Connell, T. U.; Krippner, G. Y.; Nair, A. K.; Wang, X.; Tochon-Danguy, H. J.; Donnelly, P. S.; Peter, K.; Hagemeyer, C. E. A versatile approach for the site-specific modification of recombinant antibodies using a combination of enzyme-mediated bioconjugation and click chemistry. *Angew. Chem., Int. Ed. Engl.* **2015**, *54*, 7515−7519.
(28) Beck, A.; Goetsch, L.; Dumontet, C.; Corvaïa, N. Strategies and challenges for the next generation of antibody-drug conjugates. *Nat. Rev. Drug Discovery* **2017**, *16*, 315−337.
(29) Li, D.; Zhao, X.; Zhang, L.; Li, F.; Ji, N.; Gao, Z.; Wang, J.; Kang, P.; Liu, Z.; Shi, J.; Chen, X.; Zhu, Z. ^{68}Ga-PRGD2 PET/CT in the evaluation of Glioma: a prospective study. *Mol. Pharm.* **2014**, *11*, 3923−3929.
(30) Mao, B.; Liu, C.; Zheng, W.; Li, X.; Ge, R.; Shen, H.; Guo, X.; Lian, Q.; Shen, X.; Li, C. Cyclic cRGDfk peptide and Chlorin e6 functionalized silk fibroin nanoparticles for targeted drug delivery and photodynamic therapy. *Biomaterials* **2018**, *161*, 306−320.
(31) Wang, H.; Ding, T.; Guan, J.; Liu, X.; Wang, J.; Jin, P.; Hou, S.; Lu, W.; Qian, J.; Wang, W.; Zhan, C. Interrogation of Folic Acid-Functionalized Nanomedicines: The Regulatory Roles of Plasma Proteins Reexamined. *ACS Nano* **2020**, *14*, 14779−14789.
(32) Gupta, R.; Luan, J.; Chakrabartty, S.; Scheller, E. L.; Morrissey, J.; Singamaneni, S. Refreshable Nanobiosensor Based on Organosilica Encapsulation of Biorecognition Elements. *ACS Appl. Mater. Interfaces* **2020**, *12*, 5420−5428.
(33) Brand, C.; Longo, V. A.; Groaning, M.; Weber, W. A.; Reiner, T. Development of a New Folate-Derived Ga-68-Based PET Imaging Agent. *Mol. Imaging Biol.* **2017**, *19*, 754−761.
(34) Yang, X.; Mao, Z.; Huang, Y.; Yan, H.; Yan, Q.; Hong, J.; Fan, J.; Yao, J. Reductively modified albumin attenuates DSS-Induced mouse colitis through rebalancing systemic redox state. *Redox Biol.* **2021**, *41*, 101881.
(35) Heneweer, C.; Holland, J. P.; Divilov, V.; Carlin, S.; Lewis, J. S. Magnitude of enhanced permeability and retention effect in tumors with different phenotypes: ^{89}Zr-albumin as a model system. *J. Nucl. Med.* **2011**, *52*, 625−633.
(36) Jung, K. O.; Kim, T. J.; Yu, J. H.; Rhee, S.; Zhao, W.; Ha, B.; Red-Horse, K.; Gambhir, S. S.; Pratx, G. Whole-body tracking of single cells via positron emission tomography. *Nat. Biomed. Eng.* **2020**, *4*, 835−844.
(37) Simeček, J.; Notni, J.; Kapp, T. G.; Kessler, H.; Wester, H. J. Benefits of NOPO as chelator in gallium-68 peptides, exemplified by preclinical characterization of ^{68}Ga-NOPO-c(RGDfK). *Mol. Pharm.* **2014**, *11*, 1687−1695.

https://doi.org/10.1021/acsomega.2c06720
ACS Omega 2023, 8, 4747−4755